minerals

MDPI

Article

The Effect of Grinding on Tremolite Asbestos and Anthophyllite Asbestos

Andrea Bloise [1,*], Robert Kusiorowski [2] and Alessandro F. Gualtieri [3]

1 Department of Biology, Ecology and Earth Sciences, University of Calabria, via Pietro Bucci, I-87036 Rende, CS, Italy
2 Institute of Ceramics and Building Materials, Refractory Materials Division in Gliwice, ul. Toszecka 99, 44-100 Gliwice, Poland; r.kusiorowski@icimb.pl
3 Department of Chemical and Geological Sciences, University of Modena and Reggio Emilia, I-41125 Modena, Italy; alessandro.gualtieri@unimore.it
* Correspondence: andrea.bloise@unical.it; Tel.: +39-0984-493588

Received: 4 June 2018; Accepted: 25 June 2018; Published: 28 June 2018

Abstract: The six commercial asbestos minerals (chrysotile, fibrous actinolite, crocidolite, amosite, fibrous tremolite, and fibrous anthophyllite) are classified by the IARC as carcinogenic to humans. There are currently several lines of research dealing with the inertisation of asbestos minerals among which the dry grinding process has received considerable interest. The effects of dry grinding on tremolite asbestos and anthophyllite asbestos in eccentric vibration mills have not yet been investigated. Along the research line of the mechanical treatment of asbestos, the aim of this study was to evaluate the effects of dry grinding in eccentric vibration mills on the structure, temperature stability, and fibre dimensions of tremolite asbestos from Val d'Ala, (Italy) and UICC standard anthophyllite asbestos from Paakkila mine (Finland) by varying the grinding time (30 s, 5 min, and 10 min). After grinding for 30 s to 10 min, tremolite asbestos and anthophyllite asbestos showed a decrease in dehydroxylation and breakdown temperatures due to the increase in lattice strain and the decrease in crystallinity. Moreover, after grinding up to 10 min, tremolite and anthophyllite fibres were all below the limits defining a countable fibre according to WHO.

Keywords: asbestos; tremolite; anthophyllite; grinding

1. Introduction

Tremolite $Ca_2Mg_5Si_8O_{22}(OH)_2$ asbestos and anthophyllite $Mg_7Si_8O_{22}(OH)_2$ asbestos are classified as carcinogenic substances group 1 by the IARC [1]. In fact, occupational and environmental exposure to tremolite asbestos and anthophyllite asbestos are associated with lung diseases [2–8]. In the past, large outcrops of tremolite asbestos and anthophyllite asbestos within altered ultramafic bodies have been mined in many parts of the world [9–13]. Specifically, tremolite asbestos was mined in South Korea [14], in the Teeter quarry in southeast Pennsylvania, and in the Centreville quarry in north Virginia [9,11] while anthophyllite asbestos was mainly mined in Finland and North Carolina [8,15]. In Turkey, after separating it from chrysotile (asbestos) during the milling process, tremolite was used for stuccoing the exterior surfaces of buildings [16], and a similar process was used in Cyprus [17] and all over the Middle East [18]. The mining and use of tremolite asbestos and anthophyllite asbestos were reduced compared to more commercially available types of asbestos such as chrysotile, crocidolite, and amosite [19–21]. However, despite their relatively limited use, tremolite asbestos and anthophyllite asbestos have been used in many commercial products such as cements, wall plasters, roofing materials, laboratory materials, in battery boxes, and as fillers in rubber etc. [8,21–23]. According to the existing regulations, tremolite asbestos and anthophyllite asbestos are also banned worldwide [21]. This danger

is connected with the fibrous nature of asbestos minerals, especially as a respirable form i.e., fibres with a length >5 μm, a width <3 μm, and an aspect ratio >3:1 [24]. However, tremolite asbestos and anthophyllite asbestos are considered to be contaminants of more widely used minerals such as chrysotile, talc, or vermiculite that are being exploited commercially (e.g., cement, cosmetics, asbestos-containing materials) [17,23,25]. It is important to note that chrysotile is only banned in 28% of the countries worldwide, while the other countries permit "the safe use" of chrysotile [26]. For example, tremolite asbestos was found in chrysotile outcrops in Quebec Province in Canada. The consumption of asbestos containing chrysotile has recently increased in India, which uses approximately 100,000 tons of asbestos per year, 80% of which is imported from other countries [27]. In this regard, it is worth remembering that, in India, the mining, production, and use of asbestos is very poorly regulated despite the serious risks to human health [27,28]. Furthermore, the presence of asbestos in talc has attracted much attention due to potential asbestos exposure when using products containing talc (e.g., cosmetics, filler in composites). For example, talc ore mined in upstate New York contains large amounts of both tremolite asbestos and anthophyllite asbestos, which led to high mortality rates among talc workers [12,29–31]. In this scenario, lawsuits against the multinational medical devices, pharmaceuticals, and consumer packaged goods manufacturing company that produces baby talcum powder have been instituted. According to the claimant, the use of the company's powder contributed to develop some forms of cancer [32]. Moreover, several studies have been recently carried on tremolite and anthophyllite asbestos naturally occurring in different parts of the world [8,33–35]. This is due to the relatively widespread diffusion of asbestos-containing rocks that are excavated for numerous civil engineering projects such as housing settlements, railway lines, motorways etc. e.g., [36]. Today, following the ban of its use, asbestos must be safely disposed of or made inert. In countries where asbestos minerals are banned and remediation policies are promoted, numerous attempts have been made to neutralize asbestos minerals and many studies have focused on effective asbestos inertisation methods (e.g., thermal treatment, dissolution by acid, biological treatment, thermochemical treatment) [37–43]. Amorphisation and the modification of the fibrous morphology of chrysotile asbestos by mechano-chemical treatment has been also successfully applied by several authors [44–47]. These authors showed that chrysotile asbestos completely disappeared after several hours of milling, during which part of the mechanical energy transferred to solid system is converted into heat and a part is used to destroy the crystalline framework. Bloise et al. [48] recently demonstrated that in addition to chrysotile, grinding amosite and crocidolite asbestos for up to 10 min led to almost total amorphisation and size reduction of the fibres. The reaction of tremolite when subjected to various kinds of mechanical and chemical corrosion with HCl, HNO_3, aqua regia, NaOH is described only in one paper [49], which showed that tremolite fibres were significantly modified by grinding and chemical corrosion. However, no studies have yet been carried out on tremolite asbestos and anthophyllite asbestos subjected to grinding and subsequently characterized according to degree of crystallinity, thermal behaviour, and fibre size. In this context, the aim of this study is to evaluate for the first time the effects that dry grinding process for different time in eccentric vibration mills has influence on tremolite and anthophyllite asbestos in terms of their degree of crystallinity, temperature stability, and fibre size. Using X-ray powder diffraction (XRPD), thermogravimetric analysis (TGA), and transmission electron microscopy (TEM) has given us a better understanding of the phase evolution during grinding and the changes in particle size of tremolite asbestos and anthophyllite asbestos. We believe that our study can provide new insight on how to safely dispose of asbestos through the grinding process.

2. Materials and Methods

For the study, the following mineral fibres have been used:

(1) Tremolite asbestos from Val d'Ala (Italy) with chemical formula

$$(Ca_{1.91}Na_{0.06}K_{0.01})_{1.98}(Mg_{4.71}Fe^{2+}{}_{0.22}Fe^{3+}{}_{0.08}Mn_{0.02})_{5.03}(Si_{8.01}Al_{0.02})_{8.03}O_{22.14}(OH)_{1.86}$$

This sample contains minor impurity of clinochlore and very minor impurities of antigorite and talc [50].

(2) UICC anthophyllite asbestos from Paakkila (Finland) with chemical formula:

$$Ca_{0.04}(Mg_{5.81}Fe^{2+}{}_{0.92}Fe^{3+}{}_{0.21}Mn_{0.04})_{6.98}(Si_{7.83}Al_{0.02})_{7.85}O_{21.63}(OH)_{2.37}$$

This sample contains minor impurities of clinochlore and biotite and very minor impurities of vermiculite and talc [50].

These two samples, have been extensively characterized as far as the thermal behaviour, impurity content, crystallinity, and other characteristic features [50–52]. The samples in fibrous form (1 g) were placed in a grinding container (100 mL) that incorporate an anvil ring of 1285 g and puck of 1388 g to pulverize the samples by an eccentric vibratory motion (container and ring set are made out of tungsten carbide alloy containing 9% of cobalt). The temperature never exceeds 60 °C during the grinding process. Dry grinding of the samples was conducted using Bleuler Rotary Mill (Sepor, Los Angeles, CA, USA) for 30 s, 5 min, and 10 min at a speed of 900 revolutions per min (rpm). A qualitative phase analysis of the samples before and after thermogravimetric analyses was performed by XRPD using a Bruker D8 Advance X-ray diffractometer (Bruker, Billerica, MA, USA) operating in reflection mode at 40 kV and 40 mA. Scans were recorded in the range of 3–66° 2θ, with a step size of 0.02° 2θ and a counting time of 3 s. Mineral phases were identified using DIFFRAC plus EVA software by comparing the experimental peaks with reference patterns stored in the 2005 PDF2. In the present work, the weight change and the energetic transformations were evaluated on samples by simultaneous Differential Scanning Calorimetry and Thermogravimetric Analysis (DSC/TGA: Netzsch STA 449 C Jupiter, Netzsch-Gerätebau GmbH, Selb, Germany). During DSC/TGA analysis, the samples were heated at a rate of 10 °C·min^{-1} in the 25–1100 °C temperature range under an air flow of 30 mL·min^{-1}. Approximately 20 mg of sample was used for each run. Derivative thermogravimetry (DTG), derivative differential scanning calorimetry (DDSC), exo- and endo-thermic peaks were obtained using Netzsch proteus thermal analysis software (Netzsch-Gerätebau GmbH, Selb, Germany). Instrumental precision was checked by six repeated collections on a kaolinite reference sample revealing good reproducibility (instrumental theoretical T precision of ±1.2 °C) DSC detection limit <1 μW, theoretical mass sensitivity of 0.10 μg. Size, crystallinity, structural features, and chemical composition of single fibres were determined using a Jeol JEM 1400 Plus (120 kV) transmission electron microscope (TEM, Jeol, Tokyo, Japan) equipped with Jeol large-area silicon drift detector SDD-EDS (Jeol, Tokyo, Japan) for microanalyses. Unambiguous crystallinity of individual fibres was achieved by selected area electron diffraction (SAED). For TEM investigations, the sample was put in isopropyl alcohol and then sonicated. Three drops of the obtained suspension were deposited on a Formvar carbon-coated copper grid. In order to describe the size (length and diameter) of the fibres, several hundred TEM micrographs were recorded and 20 single fibres of tremolite and anthophyllite (chemically and morphologically verified) for each grinding time (30 s, 5 min, and 10 min) were measured. Twenty fibres of both types of mineral were used to make reliable comparisons between the ground tremolite and anthophyllite samples, since after 10 min of grinding the tremolite fibres, no more than 20 fibres were observed by TEM.

3. Results

3.1. X-ray Diffraction Characterization

3.1.1. Tremolite

Figure 1a shows the X-ray diffraction patterns of tremolite asbestos ground for three different times (30 s, 5 min and 10 min). The X-ray diffraction pattern of the 30 s mechanically ground tremolite asbestos is characterized by sharp peaks (JCPDS card 44-1402) due to its high degree of crystallinity. After 5 min of grinding, all reflections are preserved even if broadened (Figure 1a). When the grinding

time is increased up to 10 min, the intensity of the peaks is reduced to the point that they are no longer distinguishable from the background (Figure 1a) except for the (110), (310), (151), and (260) reflections that were still slightly visible. This trend is mostly due to amorphisation of the sample ground for 10 min than the sample ground for 5 min. Moreover, after 5 min grinding, the diagnostic reflections of clinochlore (JCPDS card 29-0853) present as an impurity in the sample [50] are no longer visible.

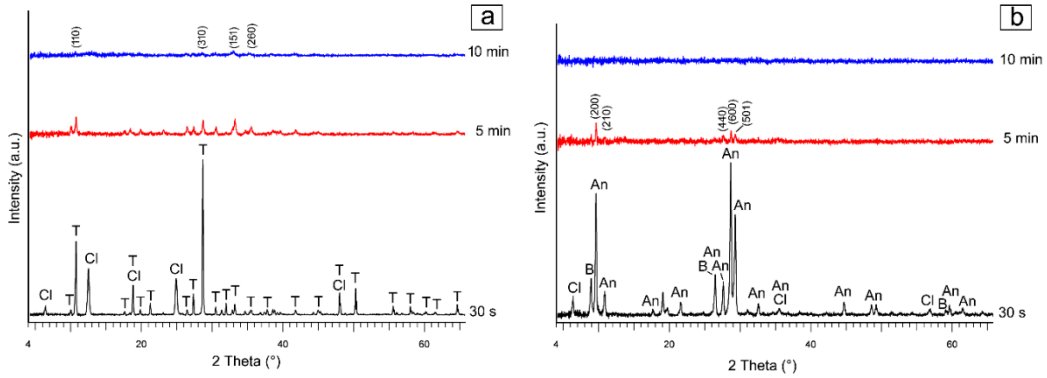

Figure 1. (**a**) X-ray powder diffraction (XRPD) patterns of the tremolite asbestos recorded after 30 s, 5 min and 10 min of grinding time; (**b**) XRPD patterns of the anthophyllite asbestos recorded after 30 s, 5 min and 10 min of grinding time. T = tremolite; Cl = clinochlore; An = anthophyllite; B = biotite.

3.1.2. Anthophyllite

After 30 s of grinding, anthophyllite asbestos is highly crystalline, with clinochlore and biotite present as impurities (Figure 1b). After 5 min of grinding, most of the anthophyllite asbestos reflections disappeared, while (200), (210), (440), (600), and (501) reflections (JCPDS card 42-0544) are less intense but preserved, suggesting that anthophyllite with lattice strain coexists with a fraction of residual crystalline fibres in the sample. After 10 min of grinding, all reflections became gradually indistinct in the pattern (Figure 1b). It is evident that no crystalline anthophyllite was detected by XRPD after 10 min grinding. Mechanical grinding also affected the structure of clinochlore (JCPDS card 24-0506) and biotite (JCPDS card 42-1437) whose characteristic reflections disappeared after 5 min of grinding (Figure 1b).

3.2. Thermal Analysis Characterization

3.2.1. Tremolite

Figure 2 shows the thermal behaviour of tremolite asbestos ground for 30 s, 5 min, and 10 min in selected temperature range. After 30 s grinding, using the maximum mass loss rate (DTG) due to the loss of hydroxyls groups when tremolite is heated up to 1100 °C, the dehydroxylation temperature of tremolite is at about 1046 °C (Table 1) even if dehydroxylation started at 1000 °C and ends at approximately 1090 °C [53,54]. After 5 min grinding, tremolite dehydroxylation occurs at a lower temperature, as shown by the DTG peak at approximately 954 °C (Figure 2), which shifts to 916 °C and becomes weaker in the sample ground for 10 min (Figure 2). DDSC confirmed the structural collapse of tremolite which occurs at lower temperatures, when the grinding time was increased from 30 s to 5 min (Table 1). Although the DDSC curve did not show detectable signals after 10 min grinding (Figure 2), when heated tremolite decomposes into pyroxene, silica and water [55] whereby the double-chain units of tremolite amphibole split into single-chain pyroxene. In fact, diopside $CaMgSi_2O_6$ (JCPDS card 38-0466) and cristobalite SiO_2 (JCPDS card 03-0257) is identified by XRPD as the main crystalline phase formed after combined thermal treatments at 1100 °C and grinding for 30 s, 5 min and 10 min (Supplementary Figure S1).

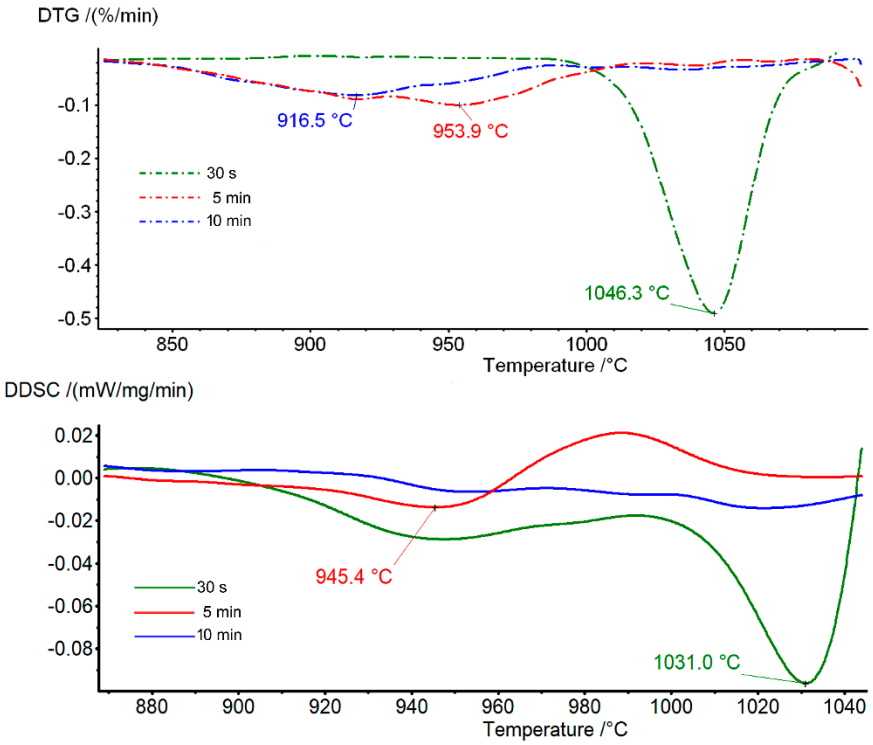

Figure 2. Derivative thermogravimetry (DTG) and derivative differential scanning calorimetry (DDSC) of tremolite asbestos after 30 s, 5 min and 10 min of grinding time.

Table 1. Dehydroxylation and breakdown peak temperatures in DTG and DDSC curves for tremolite asbestos (Tr) grinding at 30 s, 5 min and 10 min, w = weak, v = very; s = strong, endo = endothermic.

Sample (Grinding Time)	Tr 30 s	Tr 5 min	Tr 10 min
DTG (°C)	1046 endo s	954 endo w	916 endo vw
(start–end) (°C)	(1000–1090)	(930–1000)	(830–940)
DDSC (°C)	1031 endo s	945 endo w	–

3.2.2. Anthophyllite

The destruction of anthophyllite closely resembles the collapse of tremolite. In Figure 3, the broad DTG event, which starts above 800 °C and ends at approximately 900 °C, is centred at 868 °C (Table 2) and is related to the dehydroxylation of anthophyllite grinding for 30 s. This result is in agreement with the literature data [55]. The dehydroxylation temperature of anthophyllite decreases at 823 °C and starts at about 800 °C in the samples ground for 5 and 10 min (Figure 3). The broad endothermic event on DDSC curve at 850 °C (Figure 3) is related to the structural breakdown of anthophyllite grinding for 30 s, which shifts downward to approximately 816 °C for the sample ground for 5 and 10 min (Figure 3, Table 2). The product of the structural collapse is a pyroxene phase, cristobalite, and water [56]. This reaction is also observed even after grinding the sample. In fact, after heating at 1100 °C, the XRPD patterns of anthophyllite ground for 5 min and 10 min shows enstatite $MgSiO_3$ (JCPDS card 19-0606) and cristobalite SiO_2 (JCPDS card 03-0257) (Supplementary Figure S2).

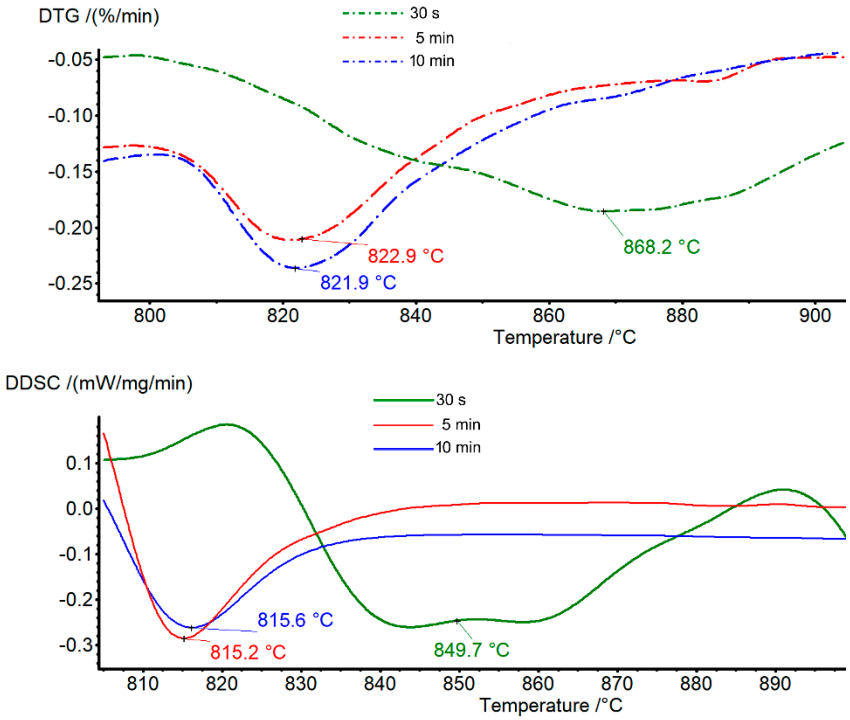

Figure 3. Derivative thermogravimetry (DTG) and derivative differential scanning calorimetry (DDSC) of anthophyllite asbestos after 30 s, 5 min, and 10 min of grinding time.

Table 2. Dehydroxylation and breakdown peak temperatures in DTG and DDSC curves for anthophyllite asbestos (Ant) grinding at 30 s, 5 min, and 10 min, w = weak, v = very; b = broad; endo= endothermic.

Sample (Grinding Time)	Ant 30 s	Ant 5 min	Ant 10 min
DTG (°C)	868 endo b	823 endo w	822 endo w
(start-end) (°C)	(810–900)	(810–850)	(810–850)
DDSC (°C)	850 endo b	815 endo w	815 endo w

3.3. TEM Characterization

Figure 4 was obtained through low magnification TEM observation to capture the whole mesh of the grid in each micrograph, as grinding time increased for tremolite (Figure 4a–c) and anthophyllite (Figure 4d–f).

3.3.1. Tremolite

After 30 s grinding, tremolite fibres exhibit a prismatic rod-shaped morphology (Figure 4a), and most fibres (70%) are >5 µm, width <3 µm (Figure 5a,b), and are therefore classified as countable fibres according to the WHO counting criteria [2]. After 5 min grinding, few fibres and numerous amorphous particles (SAED patterns with full halo rings) are detected (Figure 4b). Some fibres show impact ruptures transverse to the fibre axis, leading to a local decrease in diameter (Figure 6a).

Regarding the size of tremolite, after 5 min grinding, 100% of the fibres measured are <2 µm, and 95% have diameters <1 µm (Figure 5a,b). As grinding progressed up to 10 min, very few crystalline fibres with sharp corners and strongly reduced dimensions are detected (Figure 6b). One hundred per cent of the observed fibres are shorter than 1 µm, with 95% of diameters below 250 nm (Figure 5a,b).

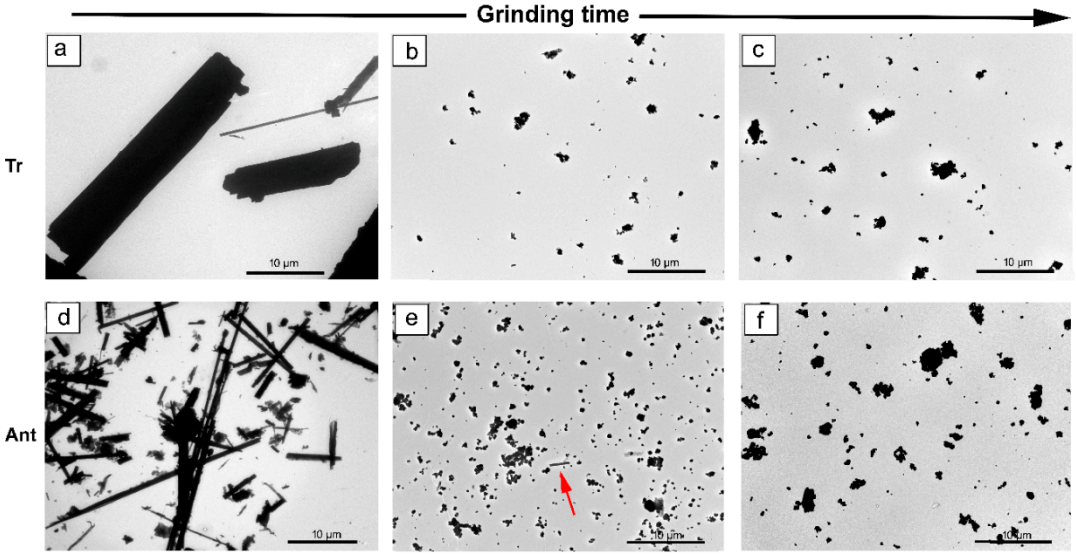

Figure 4. Transmission electron microscopy (TEM) images of: tremolite (**a**–**c**); anthophyllite (**d**–**f**); 30 s grinding (**a**,**d**); 5 min grinding (**b**,**e**); 10 min grinding (**c**,**f**).

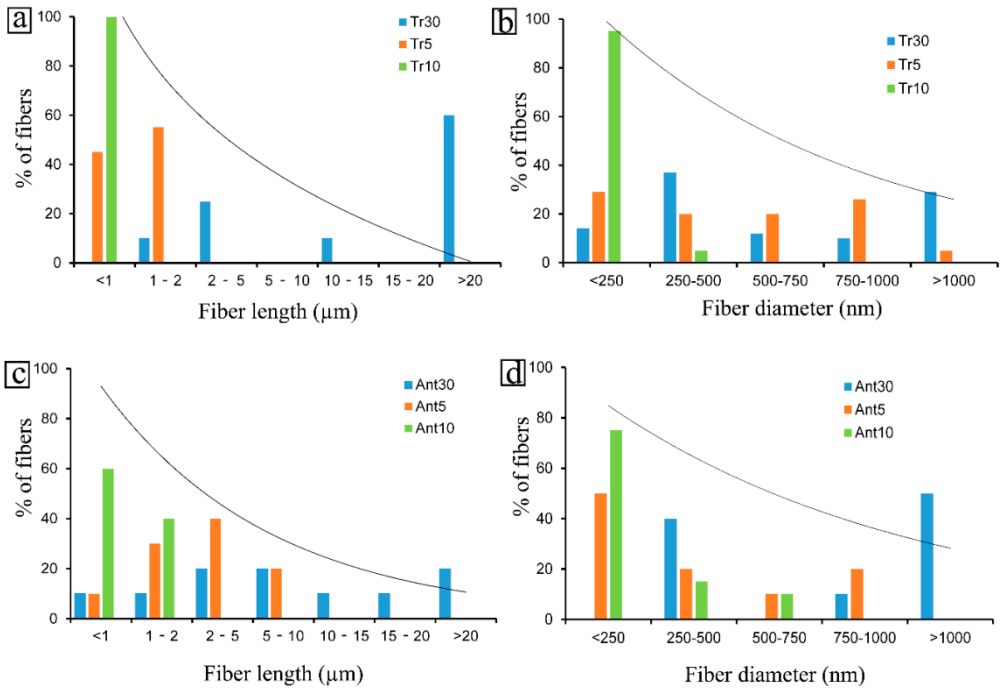

Figure 5. Size distribution of measured fibres (length and diameter) and trend line of the tremolite (**a**,**b**) and anthophyllite (**c**,**d**).

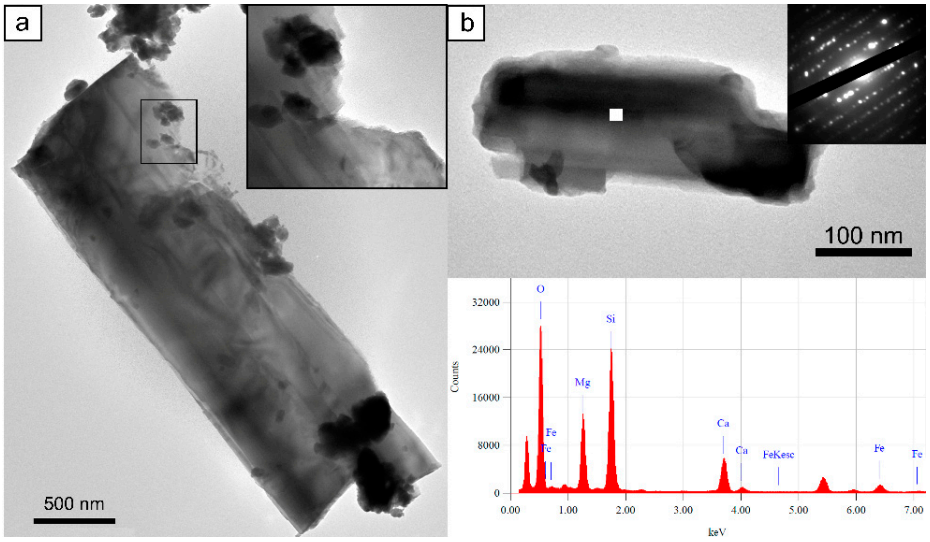

Figure 6. (**a**) TEM images of tremolite after 5 min of grinding. The black square indicates the zoom area: impact ruptures. (**b**) TEM images of tremolite after 10 min of grinding, corresponding point analysis, and selected area electron diffraction (SAED) pattern carried out on the point indicated by full white square.

3.3.2. Anthophyllite

After 30 s grinding, anthophyllite shows a needle-like crystal habit (Figure 4d) 60% of which met the size criteria defined for WHO countable fibres (Figure 5c,d) [2]. After 5 min grinding, the particle agglomerates increase with the presence of few anthophyllite fibres (Figure 4e,f), some of which are preserved while others are clearly delaminated (Figure 7a). Regarding the size, 80% of the fibres are <5 µm long with 100% of their diameters <1 µm (Figure 5c,d). As grinding increased up to 10 min, numerous amorphous agglomerates are observed (Figure 4f). Moreover, infrequent fibres with strongly rounded edges coexist with partially sharp-edged fibres (Figure 7b). One hundred per cent of the fibres are <2 µm long, with 75% of their diameters <250 nm (Figure 5c,d).

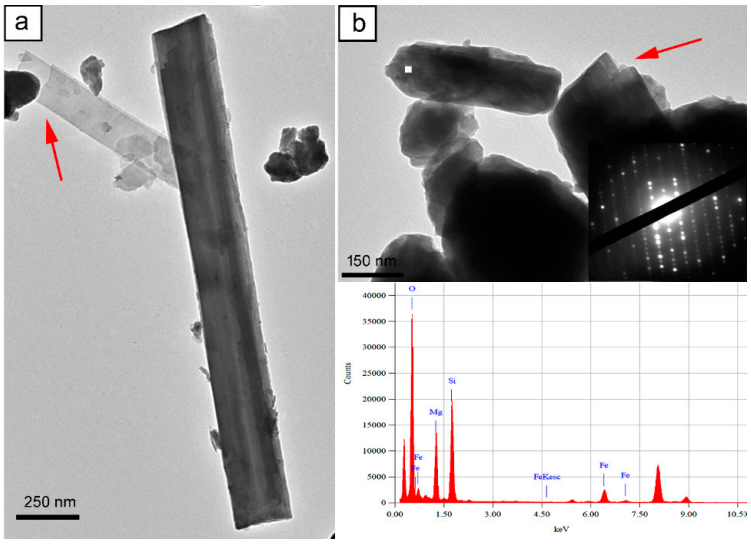

Figure 7. (**a**) TEM images of anthophyllite after 5 min of grinding. Arrows in (**a**) indicate the delaminated anthophyllite. (**b**) TEM images of anthophyllite after 10 min of grinding, corresponding point analysis and SAED pattern carried out on the point indicated by full white square. Arrows in (**b**) indicate the sharp edges of anthophyllite.

4. Discussion

The reduction of the diffraction peak intensity and the decrease of the breakdown temperatures in the DTG/DDSC curves indicate that the structure of both fibrous tremolite and anthophyllite are rapidly damaged by mechanical treatment even after 5 min grinding. Our observations on XRPD data are consistent with a decrease in crystallinity and the formation of lattice defects as grinding increased from 30 s to 10 min for both tremolite and anthophyllite samples. Notwithstanding, XRPD shows that after 5 min grinding, tremolite is still crystalline. The reduction in particle size, the formation of lattice defects, or stressed structures induced by the grinding processes caused the original maximum mass loss rate (DTG) events related to dehydroxylation to decrease, as observed for other types of asbestos such as chrysotile, amosite, and crocidolite [48]. Dehydroxylation is related to the loss of OH groups through a prototropic mechanism based on the concept of proton migration during grinding and their consequent combination with hydroxyl groups to form water molecules [48,57]. It is important to note that the effect of grinding activation is the point heating of the mineral, which causes its dehydroxylation at the contact points between the grinding medium and the mineral structure [57].

The point contact heating at specific sites leads to the achievement of the high temperatures required for dehydroxylation as follows:

$$OH^- \leftrightarrow H^+ + O^{2-}$$

Prototropy produces a water molecule as follows:

$$H^+ + OH^- \leftrightarrow H_2O$$

This reaction occurs when fibres are mechanically activated.

TGA of tremolite and anthophyllite grinding for 30 s, 5 min, and 10 min showed differences in temperature breakdown. Tremolite ranged from 1046 to 916 °C, while anthophyllite ranged from 871 to 823 °C, depending on the grinding time. However, greater reductions in dehydroxylation temperature were observed in tremolite ground for 5 min than in anthophyllite. In particular, the dehydroxylation temperature of the tremolite sample ground for 10 min is 130 °C lower than that of the sample ground for 30 s (Table 1). Anthophyllite dehydroxylation is anticipated of 46 °C for the sample ground for 10 min with respect to the sample ground for 30 s (Table 2). Moreover, 5 min of grinding before thermal treatment are sufficient to achieve the maximum decrease of temperature breakdown for both tremolite and anthophyllite asbestos, as this temperature does not change even after 10 min grinding (Table 3).

Table 3. Breakdown peak temperatures for tremolite asbestos (Tr), anthophyllite asbestos (Ant), amosite (Am), and crocidolite (Cr) grinding at 30 s, 5 min and 10 min. * After Bloise et al. [48] data from DSC curves; # data from DTG curve. w = weak, v = very; b = broad; endo= endothermic.

Grinding Time	30 s	5 min	10 min
Tr	1031 endo s	945 endo w	# 916 endo v w
Ant	850 endo b	815 endo w	815 endo w
* Am	740 endo	591 endo	536 endo
* Cr	650 endo	555 endo w	538 endo w

A similar trend is observed for chrysotile, amosite, and crocidolite [48]. We found that the decomposition temperatures of both anthophyllite and tremolite asbestos after grinding for 30 s, 5 min, and 10 min are higher than those reported for other asbestos such as amosite and crocidolite that underwent the same treatment [48] (Figure 8; Table 3).

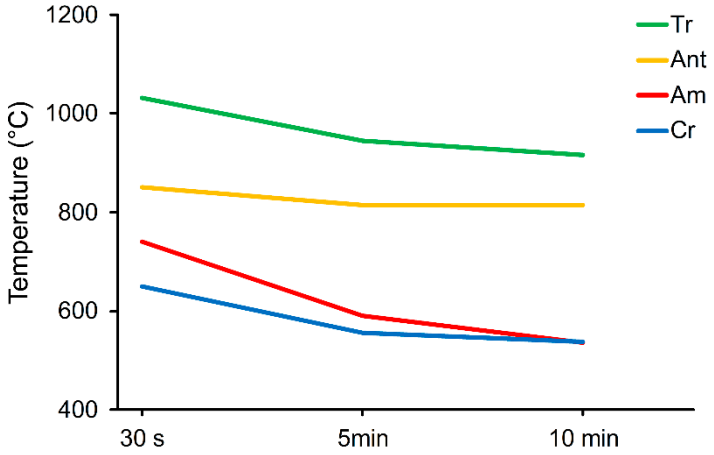

Figure 8. Changes in the temperature of amphibole asbestos breakdown in relation to the grinding time (30 s, 5 min, and 10 min).

This probably depends on the correlation between the Mg content, which is higher in anthophyllite and tremolite than in amosite and crocidolite, and the decomposition peak temperature as previously demonstrated in the literature [38,50,58]. The results of this study also prove that fibrous tremolite and anthophyllite decomposition is simultaneous with dehydroxylation as grinding increased from 30 s to 10 min. Therefore, crocidolite is the only amphibole asbestos with consecutive rather than concurrent dehydroxylation and structural breakdown processes [50,55,59] even after grinding [48].

Morphometric analyses were performed on 150 meshes observed by TEM in order to quantify the size (length and diameter) of all visible fibres, the results of which are reported in Figure 5. Regarding the length, the histograms show that after 30 s grinding 70% of tremolite and 60% of anthophyllite are generally >5 μm (Figure 5). One hundred per cent of tremolite fibres are <5 μm after 5 min grinding and even less after 10 min (Figure 5a,b). Ten minutes of grinding is required to reduce the length of 100% of the anthophyllite fibres under 5 μm. As regards diameters, grinding prompted the longitudinal splitting of both tremolite and anthophyllite fibres parallel to (110) cleavage surfaces into thinner fibrils. After 30 s grinding, all fibres are characterized by a small diameter (<3 μm) with 73% of tremolite and 50% of anthophyllite diameters <1 μm (Figure 5c,d). After grinding up to 10 min, the diameter decreased considerably with the main mode corresponding to a fibre diameter < 250 nm. In accordance with WHO fibre regulations [2], all of the tremolite fibres measured in the samples ground for 5 min were generally <5 μm long. On the other hand, 20% of anthophyllite fibres ground for 5 min are still >5 μm long while after 10 min grinding, all of the anthophyllite fibres became shorter.

5. Conclusions

For the first time, we investigated the effects that dry grinding in eccentric vibration mills produce on tremolite asbestos (Val d'Ala, Piedmont, Italy) and anthophyllite asbestos (UICC, Paakkila mine, Eastern Finland Region, Finland) in terms of crystallinity, temperature stability, and the reduction of the fibre size. Grinding tremolite and anthophyllite asbestos leads to an increase the amorphization degree and a decrease in thermal decomposition temperatures. However, the existence of rare tremolite and anthophyllite fibres preserved within the samples after 10 min grinding was detected by TEM. Tremolite proved to be the most thermally-stable amphibole asbestos even after grinding treatment. In fact, tremolite asbestos was decomposed at approximately 916 °C when it was ground for up to 10 min and after 5 min grinding all XRPD peaks were preserved. The breakdown of anthophyllite asbestos occurs at approximately 822 °C after grinding up to 10 min. On the other hand, 5 min grinding before thermal treatment are sufficient to achieve a significant reduction of the breakdown temperature for both tremolite and anthophyllite, as this temperature remains almost the same even after 10 min of grinding. This study also confirms that tremolite and anthophyllite decomposition

occurred concurrently with dehydroxylation as grinding increased. As far as the size is concerned, only 5 min grinding are required to achieve tremolite fibres with dimensions below the limits defining a countable fibre according to WHO [2], whereas 10 min of grinding are required to grind all of the anthophyllite fibres to a size < 5 µm. We believe that this study can provide novel and valuable insights into safe asbestos disposal through the grinding process and will prompt future developments of solutions for the safe disposal of asbestos containing materials.

Supplementary Materials: The following are available online at http://www.mdpi.com/2075-163X/8/7/274/s1, Figure S1: XRPD patterns after the heating at 1100 °C of tremolite asbestos ground for 30s, 5 min and 10 min. Newly formed phases: D = diopside, C = cristobalite, Figure S2: XRPD patterns after the heating at 1100 °C of anthophyllite asbestos ground for 30s, 5 min and 10 min. Newly formed phases: E = enstatite, C = cristobalite.

Author Contributions: A.B. conceived the research and performed XRPD, DSC/TG, and TEM/AEM measurements, analysed the results, and wrote the manuscript; R.K. and A.F.G. analysed the results and wrote the manuscript.

Funding: This research was funded by Italian National PROGETTO DI UNA UNITA' DI RICERCA (PRIN) 2010–2011, grant number [prot. 2010MKHT9B 004] "Interazione fra minerali e biosfera: conseguenze per l'ambiente e la salute umana".

Acknowledgments: The authors wish to thank Giorno Eugenia from Department of Chemistry and Chemical Technologies (Unical) for the support during XRPD analyses (Supplementary materials).

Conflicts of Interest: The authors declare no conflict of interest.

References

1. International Agency for Research on Cancer (IARC). *Overall Evaluations of Carcinogenicity: An Updating of IARC Monographs Volumes 1 to 42*; International Agency for Research on Cancer: Lyon, French, 1987; p. 440.
2. World Health Organization (WHO). *Asbestos and Other Natural Mineral Fibres. Environmental Health Criteria, 53*; World Health Organization: Geneva, Switzerland, 1986; p. 194.
3. Meurman, L.O.; Pukkala, E.; Hakama, M. Incidence of cancer among anthophyllite asbestos miners in Finland. *Occup. Environ. Med.* **1994**, *51*, 421–425. [CrossRef] [PubMed]
4. Karjalainen, A.; Meurman, L.O.; Pukkala, E. Four cases of mesothelioma among Finnish anthophyllite miners. *Occup. Environ. Med.* **1994**, *51*, 212–217. [CrossRef] [PubMed]
5. Luce, D.; Bugel, I.; Goldberg, P.; Goldberg, M.; Salomon, C.; Billon-Galland, M.A.; Nicolau, J.; Quénel, P.; Fevotte, J.; Brochard, P. Environmental exposure to tremolite and respiratory cancer in New Caledonia: A case-control study. *Am. J. Epidemiol.* **2000**, *151*, 259–265. [CrossRef] [PubMed]
6. Favero-Longo, S.E.; Turci, F.; Tomatis, M.; Compagnoni, R.; Piervittori, R.; Fubini, B. The effect of weathering on ecopersistence, reactivity, and potential toxicity of naturally occurring asbestos and asbestiform minerals. *J. Toxicol. Environ. Health A* **2009**, *72*, 305–314. [CrossRef] [PubMed]
7. Pugnaloni, A.; Giantomassi, F.; Lucarini, G.; Capella, S.; Bloise, A.; Di Primio, R.; Belluso, E. Cytotoxicity induced by exposure to natural and synthetic tremolite asbestos: An in vitro pilot study. *Acta Histochem.* **2013**, *115*, 100–112. [CrossRef] [PubMed]
8. Gaffney, S.H.; Grespin, M.; Garnick, L.; Drechsel, D.A.; Hazan, R.; Paustenbach, D.J.; Simmons, B.D. Anthophyllite asbestos: State of the science review. *J. Appl. Toxicol.* **2017**, *37*, 38–49. [CrossRef] [PubMed]
9. Medici, J.C. Minerals of the Fairfax quarry, Centreville, Virginia. *Mineral. Rec.* **1972**, *3*, 173–179.
10. Geyer, A.R.; Smith, R.C.I.I.; Barnes, J.H. *Mineral Collecting in Pennsylvania*; Department of Environmental Resources, Topographic and Geologic Survey, General Geology Report: Pennsylvania, PA, USA, 1976; p. 260.
11. Bernstein, L.R. *Minerals of the Washington, D.C. Area*; Maryland Geological Survey: Baltimore, MD, USA, 1980; p. 148.
12. Van Gosen, B.S.; Lowers, H.A.; Sutley, S.J.; Gent, C.A. Using the geologic setting of talc deposits as an indicator of amphibole asbestos content. *Environ. Geol.* **2004**, *45*, 920–939. [CrossRef]
13. Bloise, A.; Critelli, T.; Catalano, M.; Apollaro, C.; Miriello, D.; Croce, A.; Barrese, E.; Liberi, F.; Piluso, E.; Rinaudo, C.; et al. Asbestos and other fibrous minerals contained in the serpentinites of the Gimigliano-Mount Reventino unit (Calabria, S-Italy). *Environ. Earth Sci.* **2014**, *71*, 3773–3786. [CrossRef]
14. Addison, J.; McConnell, E.E. A review of carcinogenicity studies of asbestos and non-asbestos tremolite and other amphiboles. *Regul. Toxicol. Pharmacol.* **2008**, *52*, 1871S–S1899. [CrossRef] [PubMed]

15. Ross, M.; Virta, R.L. Occurrence, production and uses of asbestos. In *The Health Effects of Chrysotile Asbestos—Contribution of Science to Risk-Management Decisions*; Nolan, R.P., Langer, A.M., Ross, M., Wicks, F.J., Martin, R.F., Eds.; The Canadian Mineralogist, Special Publication: Ottawa, ON, Canada, 2001; Volume 5, pp. 79–88.
16. Baris, Y.I.; Bilir, N.; Artvinli, M.; Sahin, A.A.; Kalyoncu, F.; Sebastien, P. An epidemiological study in an Anatolian village environmentally exposed to tremolite asbestos. *Br. J. Ind. Med.* **1988**, *45*, 838–840. [CrossRef] [PubMed]
17. Wagner, J.C.; Chamberlain, M.; Brown, R.C.; Berry, G.; Pooley, F.D.; Davies, R.; Griffiths, D.M. Biological effects of tremolite. *Br. J. Cancer* **1982**, *45*, 352–360. [CrossRef] [PubMed]
18. Kogel, J.E.; Trivedi, N.; Barker, J.M.; Krukowski, S.T. *Industrial Minerals & Rocks: Commodities, Markets, and Uses*; Society for Mining, Metallurgy, and Exploration: Littleton, CO, USA, 2006; p. 1568.
19. Bowles, O. *Asbestos Industry*; U.S. Government Publishing Office, Bureau of Mines Bulletin: Washington, DC, USA, 1955; Volume 552, pp. 1–122.
20. Virta, R.L. *Mineral Commodity Profiles—Asbestos*; U.S. Geological Survey Circular 1255–KK: Washington, DC, USA, 2005; p. 56.
21. Gualtieri, A.F. Introduction. In *Mineral Fibres: Crystal Chemistry, Chemical-Physical Properties, Biological Interaction and Toxicity*; Gualtieri, A.F., Ed.; European Mineralogical Union: London, UK, 2017; Volume 18, pp. 1–15.
22. Huuskonen, M.S.; Ahlman, K.; Mattsson, T.; Tossavainen, A. Asbestos disease in Finland. *J. Occup. Med.* **1980**, *22*, 751–755. [PubMed]
23. Gualtieri, A.F. Mineral fibre-based building materials and their health hazards. In *Toxicity of Building Materials*; Pacheco-Torgal, F., Jalali, S., Fucic, A., Eds.; Woodhead Publishing: Cambridge, UK, 2012; pp. 166–195.
24. Directive 2009/148/EC of the European Parliament and of the Council of 30 November 2009 on the protection of workers from the risks related to exposure to asbestos at work. *Off. J. Eur. Union* **2009**, *330*, 28–36.
25. Roggli, V.L.; Coin, P. Mineralogy of asbestos. In *Pathology of Asbestos Associated Diseases*; Roggli, V., Oury, T.D., Eds.; Springer Verlag: New York, NY, USA, 2004; pp. 1–17.
26. Spasiano, D.; Pirozzi, F. Treatments of asbestos containing wastes. *J. Environ. Manag.* **2017**, *204*, 82–91. [CrossRef] [PubMed]
27. Yadav, M. *Asbestos Exposure in India*; Anchor Academic Publishing: Hamburg, Germany, 2016; p. 72.
28. Broughton, E. The Bhopal disaster and its aftermath: A review. *Environ. Health* **2005**, *4*, 1–6. [CrossRef] [PubMed]
29. Ross, M.; Smith, W.L.; Ashton, W.H. Triclinic talc and associated amphiboles from Gouverneur mining district New York. *Am. Mineral.* **1968**, *53*, 751–769.
30. Kleinfeld, M.M.D.; Messite, J.M.D.; Zaki, M.H.M.D. Mortality experiences among talc workers: A follow-up study. *J. Occup. Med.* **1974**, *16*, 345–349. [PubMed]
31. Virta, R.L. *The Talc Industry-An Overview*; U.S. Department of the Interior, Bureau of Mines: Washington, DC, USA, 1989; p. 30.
32. CNN News. Available online: https://edition.cnn.com/2018/05/24/health/johnson--johnson-talc-asbestos-verdict-california/index.html (accessed on 25 May 2018).
33. Gualtieri, A.F.; Pollastri, S.; Gandolfi, N.B.; Ronchetti, F.; Albonico, C.; Cavallo, A.; Zanetti, G.; Marini, P.; Sala, O. Determination of the concentration of asbestos minerals in highly contaminated mine tailings: An example from inactive mine waste of Cre'taz and E'marese (Valle d'Aosta, Italy). *Am. Mineral.* **2014**, *99*, 1233–1247. [CrossRef]
34. Bloise, A.; Belluso, E.; Critelli, T.; Catalano, M.; Apollaro, C.; Miriello, D.; Barrese, E. Amphibole asbestos and other fibrous minerals in the meta-basalt of the Gimigliano-Mount Reventino Unit (Calabria, South-Italy). *Rend Online Soc. Geol. Ital.* **2012**, *21*, 847–848.
35. Bloise, A.; Miriello, D. Multi-analytical approach for identifying asbestos minerals in situ. *Geosciences* **2018**, *8*, 133. [CrossRef]
36. Bloise, A.; Catalano, M.; Critelli, T.; Apollaro, C.; Miriello, D. Naturally occurring asbestos: Potential for human exposure, San Severino Lucano (Basilicata, Southern Italy). *Environ. Earth Sci.* **2017**, *76*, 648. [CrossRef]
37. Gualtieri, A.F.; Giacobbe, C.; Sardisco, L.; Saraceno, M.; Gualtieri, M.L.; Lusvardi, G.; Cavenati, C.; Zanatto, I. Recycling of the product of thermal inertization of cement-asbestos for various industrial applications. *Waste Manag.* **2011**, *31*, 91–100. [CrossRef] [PubMed]

38. Kusiorowski, R.; Zaremba, T.; Piotrowski, J.; Podwórny, J. Utilisation of cement-asbestos wastes by thermal treatment and the potential possibility use of obtained product for the clinker bricks manufacture. *J. Mater. Sci.* **2015**, *50*, 6757–6767. [CrossRef]
39. Kusiorowski, R.; Zaremba, T.; Piotrowski, J. Influence of the type of pre-calcined asbestos containing wastes on the properties of sintered ceramics. *Constr. Build. Mater.* **2016**, *106*, 422–429. [CrossRef]
40. Yamamoto, T.; Kida, A.; Noma, Y.; Terazono, A.; Sakai, S. Evaluation of thermally treated asbestos based on fiber number concentration determined by transmission electron microscopy. *J. Mater. Cycles Waste Manag.* **2016**, *20*, 214–222. [CrossRef]
41. Witek, J.; Kusiorowski, R. Neutralization of cement-asbestos waste by melting in an arc-resistance furnace. *Waste Manag.* **2017**, *69*, 336–345. [CrossRef] [PubMed]
42. Spasiano, D. Dark fermentation process as pretreatment for a sustainable denaturation of asbestos containing wastes. *J. Hazard Mater.* **2018**, *349*, 45–50. [CrossRef] [PubMed]
43. Kusiorowski, R.; Zaremba, T. The use of asbestos wastes as a fillers on Sorel cement. *Ceram. Silik.* **2018**, *62*, 31–40. [CrossRef]
44. Plescia, P.; Gizzi, D.; Benedetti, S.; Camilucci, L.; Fanizza, C.; De Simone, P.; Paglietti, F. Mechanochemical treatment to recycling asbestos-containing waste. *Waste Manag.* **2003**, *23*, 209–218. [CrossRef]
45. Inoue, R.; Kano, J.; Shimme, K.; Saito, F. Safe decomposition of asbestos by mechano-chemical reaction. *Mater. Sci. Forum* **2007**, *561*, 2257–2260. [CrossRef]
46. Hashimoto, S.; Takeda, H.; Okuda, A.; Kambayashi, A.; Honda, S.; Iwamoto, Y.; Fukuda, K. Detoxification of industrial asbestos waste by low-temperature heating in a vacuum. *J. Ceram. Soc. Jpn.* **2008**, *116*, 242–246. [CrossRef]
47. Colangelo, F.; Cioffi, R.; Lavorgna, M.; Verdolotti, L.; De Stefano, L. Treatment and recycling of asbestos-cement containing waste. *J. Hazard. Mater.* **2011**, *195*, 391–397. [CrossRef] [PubMed]
48. Bloise, A.; Catalano, M.; Gualtieri, A.F. Effect of grinding on chrysotile, amosite and crocidolite and implications for thermal treatment. *Minerals* **2018**, *8*, 135. [CrossRef]
49. Bhattacherjee, S.; Paul, A. Correlation between chemical corrosion and structural variations in fibrous tremolite. *J. Mater. Sci.* **1992**, *27*, 704–710. [CrossRef]
50. Bloise, A.; Catalano, M.; Barrese, E.; Gualtieri, A.F.; Gandolfi, N.B.; Capella, S.; Belluso, E. TG/DSC study of the thermal behaviour of hazardous mineral fibres. *J. Therm. Anal. Calorim.* **2016**, *123*, 2225–2239. [CrossRef]
51. Bloise, A.; Barca, D.; Gualtieri, A.F.; Pollastri, S.; Belluso, E. Trace elements in hazardous mineral fibres. *Environ. Pollut.* **2016**, *216*, 314–323. [CrossRef] [PubMed]
52. Ballirano, P.; Bloise, A.; Gualtieri, A.F.; Lezzerini, M.; Pacella, A.; Perchiazzi, N.; Dogan, M.; Dogan, A.U. The Crystal Structure of Mineral Fibres. In *Mineral Fibres: Crystal Chemistry, Chemical-Physical Properties, Biological Interaction and Toxicity*; Gualtieri, A.F., Ed.; European Mineralogical Union: London, UK, 2017; Volume 18, pp. 17–53.
53. Luckewicz, W. Differential thermal analysis of chrysotile asbestos in pure talc and talc containing other minerals. *J. Soc. Cosmet. Chem.* **1975**, *26*, 431–437.
54. Bloise, A.; Fornero, E.; Belluso, E.; Barrese, E.; Rinaudo, C. Synthesis and characterization of tremolite asbestos fibres. *Eur. J. Mineral.* **2008**, *20*, 1027–1033. [CrossRef]
55. Bloise, A.; Kusiorowski, R.; Lassinantti Gualtieri, M.; Gualtieri, A.F. Thermal behaviour of mineral fibres. In *Mineral Fibres: Crystal Chemistry, Chemical-Physical Properties, Biological Interaction and Toxicity*; Gualtieri, A.F., Ed.; European Mineralogical Union: London, UK, 2017; Volume 18, pp. 215–252.
56. Wittels, M.C. The structural disintegration of some amphiboles. *Am. Mineral.* **1952**, *37*, 28–36.
57. Miller, J.G.; Oulton, T.D. Prototropy in kaolinite during percussive grinding. *Clays Clay Miner.* **1970**, *18*, 313–323. [CrossRef]
58. Kusiorowski, R.; Zaremba, T.; Gerle, A.; Piotrowski, J.; Simka, W.; Adamek, J. Study on the thermal decomposition of crocidolite asbestos. *J. Therm. Anal. Calorim.* **2015**, *120*, 1585–1595. [CrossRef]
59. Freeman, A.G. The dehydroxylation behaviour of amphiboles. *Min. Mag.* **1966**, *35*, 953–957. [CrossRef]